Origin of Antibunching in Resonance Fluorescence

Lukas Hanschke,[1,2,†] Lucas Schweickert,[3,†] Juan Camilo López Carreño,[4,†] Eva Schöll,[3] Katharina D. Zeuner,[3] Thomas Lettner,[3] Eduardo Zubizarreta Casalengua,[4] Marcus Reindl,[5] Saimon Filipe Covre da Silva,[5] Rinaldo Trotta,[6] Jonathan J. Finley,[2,7] Armando Rastelli,[5] Elena del Valle,[4,8] Fabrice P. Laussy,[4,9] Val Zwiller,[3] Kai Müller,[1,2] and Klaus D. Jöns[3,*,‡]

[1]*Walter Schottky Institut and Department of Electrical and Computer Engineering, Technische Universität München, 85748 Garching, Germany*

[2]*Munich Center for Quantum Science and Technology (MCQST), 80799 Munich, Germany*

[3]*Department of Applied Physics, Royal Institute of Technology, Albanova University Centre, Roslagstullsbacken 21, 106 91 Stockholm, Sweden*

[4]*Faculty of Science and Engineering, University of Wolverhampton, Wulfruna Street, Wolverhampton WV1 1LY, United Kingdom*

[5]*Institute of Semiconductor and Solid State Physics, Johannes Kepler University Linz, 4040 Linz, Austria*

[6]*Dipartimento di Fisica, Sapienza Università di Roma, Piazzale A. Moro 1, I-00185 Roma, Italy*

[7]*Walter Schottky Institut and Physik Department, Technische Universität München, 85748 Garching, Germany*

[8]*Departamento de Física Téorica de la Materia Condensada, Universidad Autónoma de Madrid, 28049 Madrid, Spain*

[9]*Russian Quantum Center, Novaya 100, 143025 Skolkovo, Moscow Region, Russia*

(Received 25 May 2020; accepted 2 September 2020; published 23 October 2020)

Resonance fluorescence has played a major role in quantum optics with predictions and later experimental confirmation of nonclassical features of its emitted light such as antibunching or squeezing. In the Rayleigh regime where most of the light originates from the scattering of photons with subnatural linewidth, antibunching would appear to coexist with sharp spectral lines. Here, we demonstrate that this simultaneous observation of subnatural linewidth and antibunching is not possible with simple resonant excitation. Using an epitaxial quantum dot for the two-level system, we independently confirm the single-photon character and subnatural linewidth by demonstrating antibunching in a Hanbury Brown and Twiss type setup and using high-resolution spectroscopy, respectively. However, when filtering the coherently scattered photons with filter bandwidths on the order of the homogeneous linewidth of the excited state of the two-level system, the antibunching dip vanishes in the correlation measurement. Our observation is explained by antibunching originating from photon-interferences between the coherent scattering and a weak incoherent signal in a skewed squeezed state. This prefigures schemes to achieve simultaneous subnatural linewidth and antibunched emission.

DOI: 10.1103/PhysRevLett.125.170402

The prediction of photon antibunching in resonance fluorescence was made by Carmichael and Walls [1] and observed experimentally by Kimble *et al.* [2]. This initiated a flourishing and voluminous research activity on nonclassical features of light, which led to prospects of technological applications, in particular with so-called single-photon sources [3] to power quantum optical circuits or distributed quantum networks. While atomic platforms have been pioneering the investigations on the quantum nature of light, solid-state counterparts emerged as useful and versatile systems which enabled parallel and in some occasions leading fundamental studies of light-matter interactions [4,5]. Quantum dots are ideally suited as prototypical two-level quantum systems in the solid state. This is a result of their strong optical interband transitions, almost exclusive emission into the zero-phonon line and ease of integration into optoelectronic devices [3,6–8]. Moreover, the development of resonant excitation techniques [9], such as cross-polarized resonance fluorescence [10] has enabled nearly transform-limited linewidths [11], as the resonant excitation avoids the generation of free charge carriers which can lead to a fluctuating electronic environment resulting in spectral diffusion [12]. This technique has enabled multiple exciting tests of quantum optics beyond the use of quantum dots as nonclassical light sources. For example, using pulsed excitation, Rabi oscillations have been demonstrated and enabled the on-demand generation of single photons [13], entangled photon pairs [14], two-photon pulses [15], and photon number superposition states [16]. Furthermore, continuous wave excitation has led to the observation of Mollow triplets for strong driving [17] as well as coherent Rayleigh scattering in the regime of weak driving [18–20]. In the latter case, light is coherently scattered by the two-level system leading

to a subnatural linewidth of the photons which inherit the coherence of the laser [21]. While previous experimental works have indicated that the coherently scattered light exhibits antibunching [18,19], recent theoretical studies have emphasized that the antibunching is only enabled by the presence of weak incoherent emission interfering with the coherently scattered light [22]. Therefore, it was predicted that selectively transmitting the narrow coherent scattering by frequency filtering, i.e., suppressing the incoherently scattered component, would inhibit the observation of antibunching. In this Letter, we experimentally test this prediction and observe that, indeed, it is only possible to observe either subnatural linewidth or antibunching under simple resonant excitation. We provide a fundamental theoretical model giving insight to the underlying mechanism that agrees very well with our experimental results without data processing. The excellent accord between experiment and theory indicates that targeted experiments to control the balance of coherent and incoherent fractions and simultaneously achieve antibunching and subnatural linewidth, are within sight.

The quantum dots used in this study were grown by droplet etch epitaxy [23,24]. An aluminum droplet is used to dissolve an AlGaAs substrate at distinct positions to form near perfectly round holes with a diameter of ~100 nm and ~5 nm depth. These holes are filled with GaAs in a second step and capped again by AlGaAs to form single quantum dots. We focus on studying the emission of a single quantum dot under resonant excitation with a narrow linewidth (50 kHz) and frequency tunable diode laser using a scanning Fabry-Pérot interferometer with a spectral resolution of 28 MHz (see the Supplemental Material [25] for more details). While in a linear scale [Fig. 1(a)] the spectrum seems to consist of only one sharp peak, a plot in logarithmic scale [Fig. 1(b)] reveals the presence of two superimposed peaks: A sharp peak with a linewidth of 28 MHz and a broader peak with a linewidth of (890 ± 60) MHz. While the sharp peak stems from the coherent scattering and is only limited by the resolution of the scanning Fabry-Pérot interferometer, the broader peak stems from incoherent emission. Here, the observed linewidth results from emission mainly given by the Fourier limit. The ratio of the integrated peak areas is 1:2.65 and consistent with the numerical simulation of a resonantly driven two-level system [Fig. 1(c)] where the coherent scattering dominates for weak driving.

To verify the single-photon character of the quantum dot emission, we perform second-order intensity autocorrelation measurements using a Hanbury Brown and Twiss (HBT) setup connected to two superconducting nanowire single-photon detectors, with low dark count rates [30]. Our HBT setup has a time resolution of 70 ps given by the internal response function. The unfiltered emission in the Rayleigh regime shows near perfect antibunching Fig. 2 (red), confirming the single-photon character, with

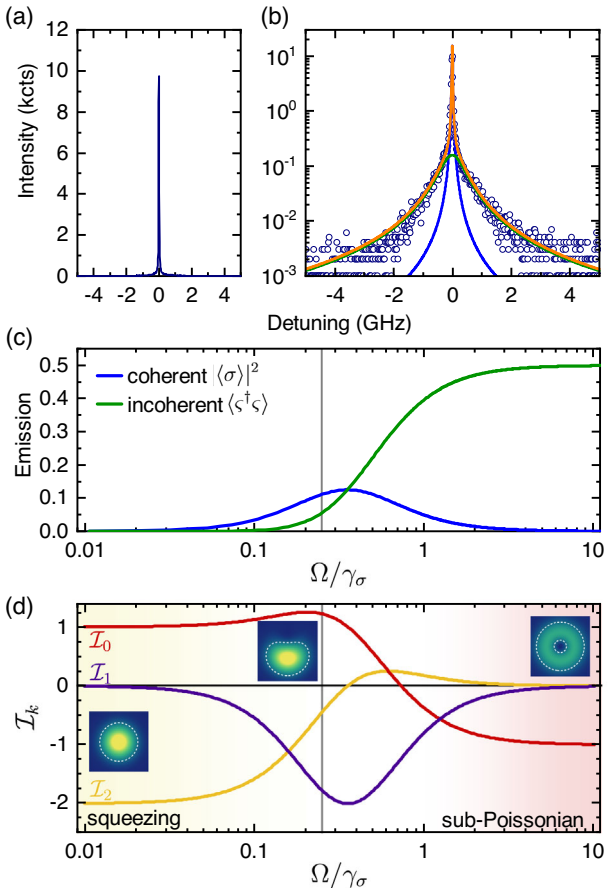

FIG. 1. (a) High resolution spectrum of the exciton transition under resonant excitation in the weak pumping regime. (b) The spectrum plotted in semilogarithmic scale reveals a second broader peak. Blue line: coherently scattered laser; green line: incoherent resonance fluorescence; orange line: cumulative peak. (c) Theoretical curves of the intensity of the coherent $|\langle\sigma\rangle|^2$ and incoherent $\langle\varsigma^\dagger\varsigma\rangle$ components as a function of the driving power. (d) Two-photon interference terms $\mathcal{I}_k$, Eqs. (4), with $k = 0, 2$ playing a role at weak and strong drivings and showing how antibunching $g^{(2)}(0) = 0$ arises from squeezing (with $\mathcal{I}_2 = -2$ on the left) or sub-Poissonian statistics of the emitter (with $\mathcal{I}_0 = -1$, on the right). The transition between the two regimes occurs through a skewing of the squeezed state whereby $\mathcal{I}_2$ gets replaced by $\mathcal{I}_1$. Insets: the Wigner representation $W_\sigma(X, Y)$ of the quantum state at weak, intermediate and strong driving, for $-1.5 \leq X, Y, \leq 1.5$ with white dashed isolines at 0 and 0.1. Note that at strong driving, W_σ becomes negative (non-Gaussian). The vertical line indicates the driving of our experiment.

a measured degree of second-order coherence of $g^{(2)}(0) = 0.022 \pm 0.011$. For this measurement we used a broad frequency filter of FWHM = 19 GHz, more than 20 times broader than the linewidth of the incoherent emission.

The light emitted by an ideal two-level system under perfect detection conditions is always antibunched, but the physical mechanism for this depends on the regime in which it is being excited. In the case of coherent driving by a laser, one can distinguish between the weak-driving

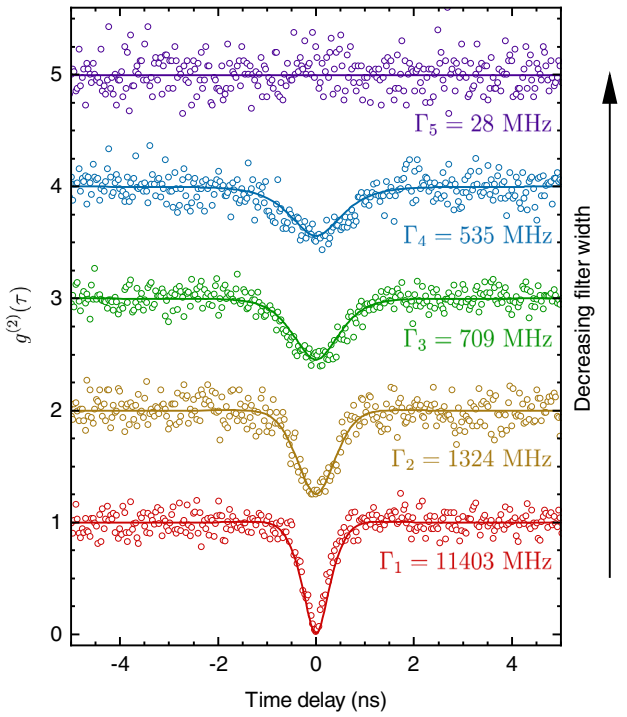

FIG. 2. Second-order intensity correlation function $g^{(2)}(\tau)$ of the quantum dot emission in the Rayleigh regime for different spectral filter widths Γ_x. With decreasing filter width, a larger portion of the incoherent component is suppressed, unbalancing the two-photon interference which produces antibunching in this regime. The experimental data is shown with empty circles, while the solid lines are obtained with the theory of frequency-resolved correlations using the parameters given in Table I.

Rayleigh regime where antibunching is due to a coherent process of absorption and reemission of the incident coherent radiation by the two-level system [31], and the strong-driving limit, where the two-level system blocks the excitation, gets saturated and emits antibunched light in the fashion of the spontaneous emission of a two-level system. While one has in mind the second mechanism when thinking of antibunching from a two-level system, the first mechanism is better understood as an interference [32]. The two-level system annihilation operator σ can be decomposed into a sum of a coherent term $\langle\sigma\rangle$ and a quantum, or incoherent, term $\varsigma \equiv \sigma - \langle\sigma\rangle$ as:

$$\sigma = \langle\sigma\rangle + \varsigma. \tag{1}$$

Note that ς is an operator, like σ, in fact it is simply σ minus its coherent part $\langle\sigma\rangle$. Their respective intensities as a function of the driving Ω and emission rate γ_σ are given by [33]

$$|\langle\sigma\rangle|^2 = \frac{4\gamma_\sigma^2\Omega^2}{(\gamma_\sigma^2 + 8\Omega^2)^2} \quad \text{and} \quad \langle\varsigma^\dagger\varsigma\rangle = \frac{32\Omega^4}{(\gamma_\sigma^2 + 8\Omega^2)^2}, \tag{2}$$

and are shown in Fig. 1(c). While the total intensity $n_\sigma \equiv \langle\sigma^\dagger\sigma\rangle$ for the sum of these two fields would typically involve an interference term $n_\sigma = |\langle\sigma\rangle|^2 + \langle\varsigma^\dagger\varsigma\rangle + 2\mathrm{Re}(\langle\sigma\rangle^*\langle\varsigma\rangle)$, in this case there is no interference since $\langle\varsigma\rangle = 0$ by construction (ς has no mean field). Higher-order photon correlations, however, do exhibit such interferences between the coherent component $\langle\sigma\rangle$, which inherits the statistics of the laser, and ς, which follows the statistics of the two-level system's quantum fluctuations. Such interferences, at the two-photon level, are quantified by coefficients $\mathcal{I}_k$ which add up to the zero-delay two-photon coherence function $g^{(2)}(0)$ as follows [34–36]:

$$g^{(2)}(0) = 1 + \mathcal{I}_0 + \mathcal{I}_1 + \mathcal{I}_2, \tag{3}$$

where:

$$\mathcal{I}_0 = \frac{\langle\varsigma^{\dagger 2}\varsigma^2\rangle - \langle\varsigma^\dagger\varsigma\rangle^2}{\langle\sigma^\dagger\sigma\rangle^2}, \tag{4a}$$

$$\mathcal{I}_1 = 4\frac{\Re[\langle\sigma\rangle^*\langle\varsigma^\dagger\varsigma^2\rangle]}{\langle\sigma^\dagger\sigma\rangle^2}, \tag{4b}$$

$$\mathcal{I}_2 = \frac{\langle :X_{\varsigma,\phi}^2: \rangle - \langle X_{\varsigma,\phi}\rangle^2}{\langle\sigma^\dagger\sigma\rangle^2}, \tag{4c}$$

and $X_{\varsigma,\phi} \equiv (e^{i\phi}\varsigma^\dagger + e^{-i\phi}\varsigma)/2$ is the ς-field quadrature which, in resonance fluorescence, gets locked at $\phi = \pi/2$. $\mathcal{I}_0$ describes the sub-Poissonian (when negative) or super-Poissonian (when positive) character of the quantum fluctuations, $\mathcal{I}_1$ its so-called anomalous moments [34,36] and $\mathcal{I}_2$ its squeezing (when negative). While it has long been known that squeezing can be present in resonance fluorescence [37,38], and its connection to antibunching is even pointed out explicitly [34,35], the nature and extent of their interrelationship in resonance fluorescence has been underappreciated, with both phenomena studied independently [4,19]. As a consequence, the opportunity for restoring or reenforcing antibunching has been overlooked. The way perfect antibunching originates from the various contributions in Eqs. (4) is shown in Fig. 1(d), where one can see the transition from $\mathcal{I}_0 = 1$ to -1 when going from weak to strong driving, which is compensated by the transition from $\mathcal{I}_2 = -2$ to 0 to keep the total (3) zero. To keep this identically zero also in the transition between these two regimes, the system develops a skewness in its squeezing through the anomalous correlation term $\mathcal{I}_1$ that overtakes $\mathcal{I}_2$, with $\langle\varsigma^\dagger\varsigma^2\rangle$ becoming nonzero (it cannot be factored into $\langle\varsigma^\dagger\varsigma\rangle\langle\varsigma\rangle$ anymore), in such a way as to satisfy $\mathcal{I}_1 = -(1 + \mathcal{I}_0 + \mathcal{I}_2)$ [32]. The numerator $\Re[\langle\sigma\rangle^*\langle\varsigma^\dagger\varsigma^2\rangle]$ can be written as $|\langle\sigma\rangle|(\langle :X_{\varsigma,\phi}^3: \rangle + \langle :X_{\varsigma,\phi}Y_{\varsigma,\phi}^2: \rangle)$ with $Y_{\varsigma,\phi} \equiv (i/2)(e^{i\phi}\varsigma^\dagger - e^{-i\phi}\varsigma)$ the other ς quadrature. This shows that, at weak driving, $\mathcal{I}_1$ becomes nonzero when the quantum state departs from a Gaussian description (squeezed

thermal state) in the transition to the strong driving regime where it acquires the full non-Gaussian character of a single-photon source that is produced by a Fock state. Indeed, the full emission at strong driving comes exclusively from the quantum part $\sigma \approx \varsigma$, with the system getting into the statistical mixture $\rho = \frac{1}{2}(|0\rangle\langle 0| + |1\rangle\langle 1|)$, with no coherence involved, $\langle\sigma\rangle = 0$. Accordingly, the sub-Poissonian statistics reaches its minimum $\mathcal{I}_0 = -1$. In the weak driving regime, antibunching is, on the opposite, due to squeezing of the quantum fluctuations ς, with the system being in a pure or skewed squeezed thermal state, with either $\mathcal{I}_2$ or $\mathcal{I}_1$ being -2, interfering with the coherent component $\langle\sigma\rangle$ to produce $g^{(2)}(0) = 0$. This can be illustrated with the Wigner representation of the quantum state, as shown by the insets in Fig. 1(d) in the three regimes of interest, where one can see how the system evolves from a Gaussian state (a displaced squeezed thermal state) to a Fock state (a ring with a distribution that admits negative values) passing by a skewed (bean-shaped) Wigner distribution at the point of our experiment. Although in the weak-driving regime, both the displacement and the ellipticity of the displaced squeezed thermal state are too small to be seen compared to the dominant thermal distribution (cf. the Supplemental Material [25]), both are necessary to produce antibunching. Counterintuitively, at weak and intermediate driving, in direct opposition to the strong-driving case, quantum fluctuations are in fact super-Poissonian, with $\mathcal{I}_0 \geq 1$. It is the interference between such superbunched quantum fluctuations with the coherence of the mean field that result in an overall antibunching, this being the two-photon counterpart of the apparent paradox of two waves adding to produce no signal (destructive interferences). This understanding of the nature of antibunching in the Rayleigh regime is important because attributing the non-Gaussian antibunching to the scattered light makes it tempting to regard the scattered light as having both the spectral feature of the laser, with a narrow linewidth, and the statistical property of a two-level system, antibunched. It has, indeed, been hailed as such in the literature [18,19,39] where these two attributes have been measured independently: excellent antibunching with a HBT setup on the one hand and narrow spectral lines with high-resolution spectroscopy on the other hand, including heterodyning and Fourier transform spectroscopy. However, because antibunching is due to some interference between the mean field $\langle\sigma\rangle$ as driven by the laser (coherent absorption) and the quantum fluctuations $\sigma - \langle\sigma\rangle$ (incoherent reemission), any tampering with the balance $\mathcal{I}_0 + \mathcal{I}_1 + \mathcal{I}_2 = -1$, for instance by frequency filtering, will result in spoiling $g^{(2)}(0) = 0$. Filtering is a fundamental process in any quantum-optical measurement, since beyond the finite bandwidth of any physical detector, a measurement that is accurate in time requires detections at all frequencies and, vice versa, spectrally resolving emission requires integration over time. To challenge the naïve picture that light coherently scattered from a two-level system is antibunched, we measure $g^{(2)}(\tau)$ for decreasing filter widths that increasingly isolate the coherent component. According to this picture, this should not affect the property of light since the "single photons" are spectrally sharp and will pass through the filter which does not block at their frequency. According to the Rayleigh picture of interferences, however, this will disrupt the balance of the $\mathcal{I}_k$ coefficients in their two-photon interference to produce antibunching. The theory shows that, for zero-delay coincidences in the weak-driving regime, the coefficients vary as a function of filtering Γ as [40]:

$$\mathcal{I}_0 = \frac{\Gamma^2}{(\Gamma + \gamma_\sigma)^2}, \qquad \mathcal{I}_1 = 0, \qquad \mathcal{I}_2 = -\frac{2\Gamma}{\Gamma + \gamma_\sigma}, \tag{5}$$

with, therefore [cf. Eq. (3)]

$$g^{(2)}(0) = \left(\frac{\gamma_\sigma}{\Gamma + \gamma_\sigma}\right)^2. \tag{6}$$

As these expressions show, filtering affects more the ς statistics than it does affect the squeezing of its quadratures. This behavior can be reproduced in the experiment by inserting a narrow spectral filter in the detection path. Measurements of $g^{(2)}(\tau)$ for different filter widths of (1550 ± 320) MHz, (780 ± 160) MHz, (390 ± 80) MHz, and 28 MHz are presented as yellow, green, blue, and purple data points in Fig. 2, respectively. The data are offset in vertical direction for clarity. Clearly, with decreasing filter width, the depth of the antibunching dip decreases until it completely vanishes.

This is in excellent agreement with our theoretical model, that describes finite τ-delay coincidences of the filtered light with an exact theory of time- and frequency-resolved photon correlations [41]. This provides an essentially perfect quantitative agreement with the data without any processing such as deconvolution, provided, however, that one also includes the effect of the anomalous moment term $\mathcal{I}_1$, which bridges between the weak and strong driving regimes. Indeed, Ω was not so low in the experiment—in the interest of collecting enough signal in presence of filtering—as to realize an ideal squeezed state to interfere with the coherent fraction to produce the antibunching, but relied on a distorted, skewed version of the squeezed state in its transition towards the non-Gaussian, strong-driving regime where squeezing has disappeared altogether. This term brings quantitative deviations which are necessary to take into account to provide an exact match with the data. The unfiltered case, for instance, sees the vanishing-driving two-photon statistics $g^{(2)}(\tau) = [1 - \exp(-\gamma_\sigma\tau/2)]^2$ turn into

$$g^{(2)}(\tau) = 1 - e^{-3\gamma_\sigma\tau/4}\left[\cosh\left(\frac{R\tau}{4}\right) + \frac{3\gamma_\sigma}{R}\sinh\left(\frac{R\tau}{4}\right)\right], \tag{7}$$

TABLE I. Summary of the parameters used to fit the experimental data. The filters data are taken from the fabricant's data sheet, but are known to be typically measured in excess of their specified value.

Parameter	γ_σ	Ω	Γ_1	Γ_2	Γ_3	Γ_4	Γ_5
Fitting (MHz)	900	225	11 403	1324	709	535	28
Data (MHz) (Error)	890 (60)	198 (7)	19 000 (500)	1550 (320)	780 (160)	390 (80)	28 (6)

at non-negligible driving, with $R = \sqrt{\gamma_\sigma^2 - 64\Omega^2}$. Using this and numerically exact filtered counterparts, with a global fitting that only varies the filters widths and globally optimises the driving strength Ω and the two-level's decay rate $\gamma_\sigma = 900$ MHz (cf. Table I), we obtain the solid lines shown in Fig. 2, providing an excellent quantitative agreement with highly constrained fitting parameters. From this data, one can extract the zero-delay coincidence and compare it to the theory, i.e., both Eq. (6), shown in dashed red in Fig. 3, or to the finite Ω counterpart that skews the squeezing, and whose expression is too bulky to be written here [42], but is given in the Supplemental Material [25], Eq. (14). This also yields an excellent agreement with the experimental data, which confirms that filtering spoils antibunching according to the scenario we have explained of perturbing the interference of the squeezed fluctuations with the coherent signal, and that the experiment is clean and fundamental enough to be reproduced exactly by including nonvanishing driving features, without any further signal analysis or data processing.

In summary, we have shown that the emission from a two-level quantum system driven in the Rayleigh regime does not simultaneously yield subnatural linewidth and single-photon characteristics. When keeping only the subnatural linewidth part of the spectrum by frequency filtering, we do not observe antibunching in our second-order intensity correlation measurement. The narrower the spectral filtering, i.e., the fewer incoherently scattered photons we detect, the weaker the antibunching dip, which ultimately

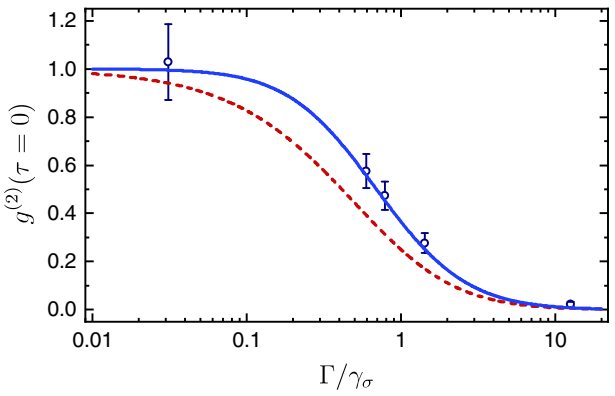

FIG. 3. Loss of antibunching in the Rayleigh regime due to filtering Γ. Dashed-red line, the limit of vanishing driving, Eq. (6), and solid-blue line, the case of small but finite driving Ω, see the Supplemental Material [25] Eq. (14). Our experimental data fits perfectly with the theoretical prediction.

results in Poissonian photon statistics. These results, which disclose a perfect agreement with a fundamental theory of time and frequency resolved photon correlations, with no post-processing of the raw experimental data, are only the first step towards a full exploitation of its consequences. In particular, since the interference involves a coherent field, it is technically possible to restore it fully in presence of filtering or, which is equivalent, detection, simply by introducing externally the coherent fraction that is missing or, in this case, is in excess. This is done by destructive interferences of the coherent signal, without perturbing the quantum fluctuations. As a result, one should indeed obtain a subnatural, laser-sharp, photon emission that is also perfectly antibunched [22]. There are still other interesting features in this regime, such as a plateau in the time-resolved photon correlations. This also pauses the question of the possible generalization and relevance of such results to other scattering schemes of single-photon generation, such as Raman single-photon sources [43]. Such followup works are in the wake of our present findings.

This project has received funding from the European Union's Horizon 2020 research and innovation program under Grants Agreement No. 820423 (S2QUIP) and No. 899814 (Qurope), the European Research Council (ERC) under the European Union's Horizon 2020 Research and Innovation Programme (SPQRel, Grant Agreement No. 679183), Austrian Science Fund (FWF): P 29603, P 30459, the Linz Institute of Technology (LIT) and the LIT Lab for secure and correct systems, supported by the State of Upper Austria, the German Federal Ministry of Education and Research via the funding program Photonics Research Germany (Contract No. 13N14846), Q.Com (Project No. 16KIS0110) and Q.Link.X (16KIS 0874), the DFG via Project (SQAM) No. F1947/4-1, the Nanosystem Initiative Munich, the Munich Center for Quantum Science and Technology (MCQST), the Knut and Alice Wallenberg Foundation grant "Quantum Sensors," the Swedish Research Council (VR) through the VR grant for international recruitment of leading researchers (Ref: 2013-7152), and Linnæus Excellence Center ADOPT. K. M. acknowledges support from the Bavarian Academy of Sciences and Humanities. K. D. J. acknowledges funding from the Swedish Research Council (VR) via the starting Grant HyQRep (Ref. No. 2018-04812) and The Göran Gustafsson Foundation (SweTeQ). A. R. acknowledges fruitful discussions with Y. Huo, G. Weihs, R. Keil, and S. Portalupi.

Note added—Recently, we became aware of a similar work [44].

*Corresponding author.
klaus.joens@uni-paderborn.de
†L. H., L. S., and J. C. L. C. contributed equally to this work.
‡Present address: Department of Physics, Paderborn University, 33098 Paderborn, Germany.

[1] H. J. Carmichael and D. F. Walls, J. Phys. B **9**, L43 (1976).
[2] H. J. Kimble, M. Dagenais, and L. Mandel, Phys. Rev. Lett. **39**, 691 (1977).
[3] P. Senellart, G. Solomon, and A. White, Nat. Nanotechnol. **12**, 1026 (2017).
[4] C. H. Schulte, J. Hansom, A. E. Jones, C. Matthiesen, C. Le Gall, and M. Atature, Nature (London) **525**, 222 (2015).
[5] F. P. Laussy, Nat. Mater. **16**, 398 (2017).
[6] R. Trivedi, K. A. Fischer, J. Vučković, and K. Müller, Adv. Quantum Technol. **3**, 1900007 (2020).
[7] P. Borri, W. Langbein, S. Schneider, U. Woggon, R. L. Sellin, D. Ouyang, and D. Bimberg, Phys. Rev. Lett. **87**, 157401 (2001).
[8] A. J. Brash, J. Iles-Smith, C. L. Phillips, D. P. S. McCutcheon, J. O'Hara, E. Clarke, B. Royall, L. R. Wilson, J. Mørk, M. S. Skolnick, A. M. Fox, and A. Nazir, Phys. Rev. Lett. **123**, 167403 (2019).
[9] A. Muller, E. B. Flagg, P. Bianucci, X. Y. Wang, D. G. Deppe, W. Ma, J. Zhang, G. J. Salamo, M. Xiao, and C. K. Shih, Phys. Rev. Lett. **99**, 187402 (2007).
[10] A. V. Kuhlmann, J. Houel, D. Brunner, A. Ludwig, D. Reuter, A. D. Wieck, and R. J. Warburton, Rev. Sci. Instrum. **84**, 073905 (2013).
[11] A. V. Kuhlmann, J. H. Prechtel, J. Houel, A. Ludwig, D. Reuter, A. D. Wieck, and R. J. Warburton, Nat. Commun. **6**, 8204 (2015).
[12] D. Chen, G. R. Lander, K. S. Krowpman, G. S. Solomon, and E. B. Flagg, Phys. Rev. B **93**, 115307 (2016).
[13] Y. M. He, Y. He, Y. J. Wei, D. Wu, M. Atatüre, C. Schneider, S. Höfling, M. Kamp, C. Y. Lu, and J. W. Pan, Nat. Nanotechnol. **8**, 213 (2013).
[14] M. Müller, S. Bounouar, K. D. Jöns, M. Glässl, and P. Michler, Nat. Photonics **8**, 224 (2014).
[15] K. A. Fischer, L. Hanschke, J. Wierzbowski, T. Simmet, C. Dory, J. J. Finley, J. Vučkovič, and K. Müller, Nat. Phys. **13**, 649 (2017).
[16] J. C. Loredo, C. Antón, B. Reznychenko, P. Hilaire, A. Harouri, C. Millet, H. Ollivier, N. Somaschi, L. De Santis, A. Lemaître, I. Sagnes, L. Lanco, A. Auffèves, O. Krebs, and P. Senellart, Nat. Photonics **13**, 803 (2019).
[17] E. B. Flagg, A. Muller, J. W. Robertson, S. Founta, D. G. Deppe, M. Xiao, W. Ma, G. J. Salamo, and C. K. Shih, Nat. Phys. **5**, 203 (2009).
[18] H. S. Nguyen, G. Sallen, C. Voisin, P. Roussignol, C. Diederichs, and G. Cassabois, Appl. Phys. Lett. **99**, 261904 (2011).
[19] C. Matthiesen, A. N. Vamivakas, and M. Atatüre, Phys. Rev. Lett. **108**, 093602 (2012).
[20] K. Konthasinghe, J. Walker, M. Peiris, C. K. Shih, Y. Yu, M. F. Li, J. F. He, L. J. Wang, H. Q. Ni, Z. C. Niu, and A. Muller, Phys. Rev. B **85**, 235315 (2012).
[21] C. Matthiesen, M. Geller, C. H. Schulte, C. Le Gall, J. Hansom, Z. Li, M. Hugues, E. Clarke, and M. Atatüre, Nat. Commun. **4**, 1600 (2013).
[22] J. C. López Carreno, E. Zubizarreta Casalengua, F. P. Laussy, and E. Del Valle, Quantum Sci. Technol. **3**, 045001 (2018).
[23] C. Heyn, A. Stemmann, T. Köppen, C. Strelow, T. Kipp, M. Grave, S. Mendach, and W. Hansen, Appl. Phys. Lett. **94**, 183113 (2009).
[24] Y. H. Huo, A. Rastelli, and O. G. Schmidt, Appl. Phys. Lett. **102**, 152105 (2013).
[25] See the Supplemental Material at http://link.aps.org/supplemental/10.1103/PhysRevLett.125.170402 for further details on the Wigner representation, frequency filtering and the experimental setup, which includes Refs. [26–29].
[26] H. J. Carmichael, H. M. Castro-Beltran, G. T. Foster, and L. A. Orozco, Phys. Rev. Lett. **85**, 1855 (2000).
[27] R. J. Glauber, Phys. Rev. Lett. **10**, 84 (1963).
[28] H. S. Nguyen, G. Sallen, C. Voisin, P. Roussignol, C. Diederichs, and G. Cassabois, Phys. Rev. Lett. **108**, 057401 (2012).
[29] D. Huber, B. U. Lehner, D. Csontosová, M. Reindl, S. Schuler, S. F. Covre da Silva, P. Klenovský, and A. Rastelli, Phys. Rev. B **100**, 235425 (2019).
[30] L. Schweickert, K. D. Jöns, K. D. Zeuner, S. F. Covre Da Silva, H. Huang, T. Lettner, M. Reindl, J. Zichi, R. Trotta, A. Rastelli, and V. Zwiller, Appl. Phys. Lett. **112**, 093106 (2018).
[31] W. Heitler, *The Quantum Theory of Radiation* (Oxford University Press, London, 1954).
[32] E. Zubizarreta Casalengua, J. C. López Carreño, F. P. Laussy, and E. del Valle, Laser Photonics Rev. **14**, 1900279 (2020).
[33] P. Meystre and M. Sargent, *Elements of Quantum Optics* (Springer-Verlag Berlin Heidelberg, Berlin Heidelberg, 2007), pp. 1–507.
[34] L. Mandel, Phys. Rev. Lett. **49**, 136 (1982).
[35] H. J. Carmichael, Phys. Rev. Lett. **55**, 2790 (1985).
[36] W. Vogel, Phys. Rev. Lett. **67**, 2450 (1991).
[37] D. F. Walls and P. Zoller, Phys. Rev. Lett. **47**, 709 (1981).
[38] R. Loudon, Opt. Commun. **49**, 24 (1984).
[39] J. T. Höffges, H. W. Baldauf, T. Eichler, S. R. Helmfrid, and H. Walther, Opt. Commun. **133**, 170 (1997).
[40] E. Zubizarreta Casalengua, J. C. López Carreño, F. P. Laussy, and E. del Valle, Phys. Rev. A **101**, 063824 (2020).
[41] E. del Valle, A. Gonzalez-Tudela, F. P. Laussy, C. Tejedor, and M. J. Hartmann, Phys. Rev. Lett. **109**, 183601 (2012).
[42] J. C. López Carreño and F. P. Laussy, Phys. Rev. A **94**, 063825 (2016).
[43] B. C. Pursley, S. G. Carter, M. K. Yakes, A. S. Bracker, and D. Gammon, Nat. Commun. **9**, 115 (2018).
[44] C. L. Phillips, A. J. Brash, D. P. S. McCutcheon, J. Iles-Smith, E. Clarke, B. Royall, M. S. Skolnick, A. M. Fox, and A. Nazir, Phys. Rev. Lett. **125**, 043603 (2020).